Author Manuscript

Author Manuscript

Author Manuscript

Author Manuscript

HHS Public Access

Author manuscript

J Biomed Mater Res A. Author manuscript; available in PMC 2015 January 19.

Published in final edited form as:

J Biomed Mater Res A. 2014 January ; 102(1): 234–246. doi:10.1002/jbm.a.34671.

Polypropylene Surgical Mesh Coated with Extracellular Matrix Mitigates the Host Foreign Body Response

Matthew T. Wolf[a,c], **Christopher A. Carruthers**[a,c], **Christopher L. Dearth**[b,c], **Peter M. Crapo**[c,d], **Alexander Huber**[c], **Olivia A. Burnsed**[e], **Ricardo Londono**[c], **Scott A. Johnson**[c], **Kerry A. Daly**[c], **Elizabeth C. Stahl**[a,c], **John M. Freund**[a,c], **Christopher J. Medberry**[a,c], **Lisa E. Carey**[a,c], **Alejandro Nieponice**[b,c], **Nicholas J. Amoroso**[a,c], and **Stephen F. Badylak**[a,b,c]

[a]Department of Bioengineering, University of Pittsburgh, Pittsburgh, PA

[b]Department of Surgery, University of Pittsburgh, Pittsburgh, PA

[c]McGowan Institute for Regenerative Medicine, University of Pittsburgh, Pittsburgh, PA

[d]C. R. Bard Inc., Warwick, RI

[e]Department of Biomedical Engineering, Georgia Institute of Technology, Altanta, GA

Abstract

Surgical mesh devices composed of synthetic materials are commonly used for ventral hernia repair. These materials provide robust mechanical strength and are quickly incorporated into host tissue; factors which contribute to reduced hernia recurrence rates. However, such mesh devices cause a foreign body response with the associated complications of fibrosis and patient discomfort. In contrast, surgical mesh devices composed of naturally occurring extracellular matrix (ECM) are associated with constructive tissue remodeling, but lack the mechanical strength of synthetic materials. A method for applying a porcine dermal ECM hydrogel coating to a polypropylene mesh is described herein with the associated effects upon the host tissue response and biaxial mechanical behavior. Uncoated and ECM coated heavy-weight BARD™ Mesh were compared to the light-weight ULTRAPRO™ and BARD™ Soft Mesh devices in a rat partial thickness abdominal defect overlay model. The ECM coated mesh attenuated the pro-inflammatory response compared to all other devices, with a reduced cell accumulation and fewer foreign body giant cells. The ECM coating degraded by 35 days, and was replaced with loose connective tissue compared to the dense collagenous tissue associated with the uncoated polypropylene mesh device. Biaxial mechanical characterization showed that all of the mesh devices were of similar isotropic stiffness. Upon explantation, the light-weight mesh devices were more compliant than the coated or uncoated heavy-weight devices. The present study shows that an ECM coating alters the default host response to a polypropylene mesh, but not the mechanical properties in an acute *in vivo* abdominal repair model.

All correspondence should be addressed to: Stephen F. Badylak, DVM, PhD, MD, (badylaks@upmc.edu). 450 Technology Drive, Suite 300. University of Pittsburgh, Pittsburgh, PA 15219, USA.

Author Manuscript Author Manuscript Author Manuscript Author Manuscript

Keywords

Extracellular Matrix (ECM); polypropylene; surgical mesh; coated surgical mesh; foreign body response

1. Introduction

Non-degradable synthetic mesh materials, including polypropylene, polyethylene, and polyethylene terephthalate (PET), are routinely used for abdominal and inguinal hernia repair. Knitted polypropylene, the most commonly used non-degradable synthetic mesh material, was first described for abdominal wall repair in 1963 and found to significantly reduce hernia recurrence rates.[1,2] The clinical use of polypropylene surgical mesh materials has steadily increased with over 1 million polypropylene mesh devices implanted worldwide each year,[3] and this material is currently considered one of the standard biomaterials for hernia repair. The robust mechanical properties and host soft tissue response to polypropylene mesh materials and similar non-degradable synthetic materials have been well characterized.[4–8] These mesh materials are quickly incorporated into the adjacent host tissue where they elicit a chronic pro-inflammatory response, with subsequent formation of dense fibrous tissue within and around the mesh material.[3,5,9] The fibrous connective tissue deposition, though contributing to the overall strength of the surgical repair, creates a compliance mismatch between the mesh and abdominal wall; a phenomenon associated with pain and discomfort for the recipient.[9–11] Several strategies have been investigated to minimize the fibrotic response to synthetic mesh materials including alterations in the mesh fiber composition, reduction of mesh surface area (referred to as a “lightweight” mesh),[3,5,12–14] and application of bioactive coatings.

Non-synthetic materials have been investigated for hernia repair. Surgical mesh materials composed of naturally occurring allogeneic or xenogeneic extracellular matrix (ECM) have been used as an alternative to synthetic materials to abrogate the foreign body response, prevent infection, and minimize or avoid excessive fibrosis.[15–19] Though ECM mesh materials are typically degradable[20] (i.e., if not chemically crosslinked) and lack the robust mechanical properties of polypropylene,[21–23] they promote the deposition of site appropriate soft tissue such as adipose tissue, muscle tissue, and/or vascularized reticular connective tissue rather than dense fibrous tissue.[18,24] Development of a hybrid polypropylene-ECM material that could capitalize on both the desirable mechanical properties of the synthetic non-degradable polypropylene and the tissue remodeling properties of the naturally occurring ECM would represent a step forward in biomaterial engineering.

The present study investigated the host response to a heavy-weight polypropylene mesh coated with a hydrogel form of porcine dermal ECM. An uncoated heavy-weight mesh and two light-weight synthetic mesh devices were included as a comparison to the ECM modified heavyweight mesh. The *in vivo* remodeling response and biomechanics were evaluated in a rat partial thickness abdominal wall defect model.

Author Manuscript Author Manuscript Author Manuscript Author Manuscript

2. Materials and Methods

2.1. Overview of experimental design and test articles

BARD™ Mesh, a heavy-weight polypropylene surgical mesh (C.R. BARD-Davol Inc., Providence, RI), was coated with a hydrogel composed of dermal ECM. The mechanical properties and host soft tissue response following implantation in a rat partial abdominal wall defect were compared to those of a non-coated heavy-weight polypropylene surgical mesh and two light-weight surgical mesh devices. The light-weight meshes used in this study were Ethicon ULTRAPRO™ (Ethicon Inc., San Angelo, TX), a polypropylene/ monocryl composite mesh, and BARD™ Soft Mesh, a polypropylene mesh.

2.2. Dermal ECM preparation and polypropylene mesh coating

Dermal ECM was prepared as previously described[25] from full thickness skin harvested from market weight (approximately 110 kg) pigs. In brief, subcutaneous fat and epidermis were removed by mechanical delamination followed by treatment with 0.25% trypsin (Thermo Fisher Scientific, Waltham, MA) for 6 hours, 70% ethanol for 10 hours, 3% H_2O_2 for 15 minutes, 1% Triton X-100 (Sigma-Aldrich, St. Louis, MO) in 0.26% EDTA/0.69% Tris for 6 hours with a solution change for an additional 16 hours, 0.1% peracetic acid/4% ethanol (Rochester Midland Corp., Rochester, NY) for 2 hours. Water washes were performed between each chemical change with alternating water and phosphate buffered saline (PBS) washes following the final step. All chemical exposures were conducted under agitation on an orbital shaker at 300 RPM.

Dermal ECM was then frozen, lyophilized, and comminuted into a 40 mesh powder. The dermal ECM powder was solubilized as previously described[26,27] by partial enzymatic digestion in a 1 mg/ml pepsin (Sigma-Aldrich) solution in 0.01 N HCl for 48 hours at a concentration of 10 mg ECM/ml solution (dry wt/vol). Solubilized dermal ECM was brought to physiologic pH and salt concentration while on ice by adding 1/9 the digest volume of 10X PBS, 1/10 the volume of 0.1 N NaOH, and then further diluted to 8 mg ECM/ml with 1X PBS. The neutralized dermal ECM digest was immediately added to a square plastic dish and 2 cm × 3 cm pieces of pre-cut polypropylene mesh were suspended in the solution. The viscosity of the digest was sufficient for the mesh to remain in suspension until gelation had occurred. The neutralized digest and polypropylene mesh were then placed in a non-humidified incubator at 37 °C for approximately 30–45 minutes until the dermal ECM digest formed a hydrogel (approximately 4.5 mm total thickness) around the mesh (approximately 0.66 mm mesh thickness) and between the fibers of the polypropylene mesh. The dermal ECM hydrogel embedded mesh was then air dried at 37°C overnight to complete the coating process (approximately 0.68 mm ECM coated mesh thickness). Stability of the ECM coating was determined by placing ECM coated meshes in PBS at 37°C for 3 × 15 minute washes followed by immersion for 24 hours in PBS and subsequent examination for evidence of delamination of the ECM from the polypropylene. All devices used for *in vivo* implantation were terminally sterilized with ethylene oxide.

Author Manuscript Author Manuscript Author Manuscript Author Manuscript

2.3. Scanning electron microscopy

Mesh fiber geometry and surface characteristics were evaluated with scanning electron microscopy (SEM). The ECM coated mesh was hydrated in PBS and fixed in 2.5% glutaraldehyde for scanning electron microscopy. ECM coated meshes were then washed with PBS, dehydrated in a graded series of ethanol, and dried in hexamethyldisilazane (Thermo-Fisher Scientific). The non-coated polypropylene mesh materials did not require fixation or dehydration. The ECM coated mesh, uncoated BARD™, ULTRAPRO™, and BARD™ Soft, meshes were mounted onto aluminum stubs and then sputter coated (Sputter Coater 108 Auto, Cressington Scientific Instruments, Watford, UK) with a 3.5 nm thick gold/palladium alloy. The meshes were then imaged with a scanning electron microscope (JEOL JSM6330f, JEOL Ltd., Peabody, MA) at a 3.0 kV accelerating voltage.

2.4. Mesh in vivo implantation

Mesh materials were used to repair an *in vivo* model of abdominal wall injury to evaluate mesh remodeling response and biomechanical properties.[16,18] Female Sprague-Dawley rats (250–300 g) were anesthetized with 2–3% isofluorane and ventral midline skin incision was made. A 1 cm × 1 cm partial thickness paramedian defect was created by removing the internal and external oblique muscles and leaving the *transversalis fascia* and peritoneum intact. The defects were either left untreated as controls or were overlayed with 2 cm × 3 cm mesh test articles centered over the defect area, with the 3 cm edge of the mesh parallel to midline along the edge of the *rectus abdominus* as shown in Figure 1A–B. Mesh placement was consistent by aligning the stiffer axis perpendicular to the midline (i.e. along the abdominal wall circumferential direction), and the more compliant axis parallel to the midline (i.e. along the rostral to caudal, or longitudinal direction). Each mesh possessed anisotropic mechanical behavior, in which the mesh was stiffer in one direction compared to the perpendicular direction under uniaxial loads (as shown in the results section). Mesh fixation to the abdominal wall was achieved using single interrupted 4-0 Prolene sutures (Ethicon) at the 4 corners of the mesh with 2 additional sutures at the midpoint of the 3 cm edge of the mesh. Each rat was implanted with 2 randomly assigned mesh devices, one per side. The skin incision was then closed with 4-0 Vicryl (Ethicon) suture and the animals were allowed to recover and ambulate normally. Animals were sacrificed after 3, 7, 14, or 35 days of implantation (Figure 1C), after which time, the mesh and associated muscle tissue was explanted for either histologic (n=4 animals per device and time point) or biomechanical characterization (n=8 animals per device at the 35 day time point).

2.5. Quantitative histologic analysis and immunolabeling

A quantitative histomorphometric scoring system was used to evaluate the host response to the implanted mesh materials at each time point as summarized in Table 1. Mesh-tissue explants were immediately fixed with formalin, embedded in paraffin, sectioned (5 μm), mounted onto microscope slides, and stained with hematoxylin and eosin (H&E). A total of 6 high magnification images (400X) were acquired by blinded observers for each H&E stained section; 3 images of the mesh fiber/tissue interface and 3 images of the deposited tissue between mesh fibers. The mesh fiber/tissue interface images were positioned at the edge of mesh fiber bundles such that the inflammatory response to the mesh was visible

Author Manuscript Author Manuscript Author Manuscript Author Manuscript

within the field of view. The mesh fiber/tissue interface images were quantified for 2 criteria: the thickness of the dense cell accumulation at the fiber surface (reported as number of cell layers away from the mesh fiber) and the total number of multinucleate foreign body giant cells surrounding the mesh fiber in each image. The images of the tissue between mesh fibers were acquired at the midpoint between adjacent mesh fiber bundles and were quantified for 2 criteria; the total number of mononuclear cells per image (rounded to the nearest 50) and the total number of blood vessels (with identifiable lumen and red blood cells). All quantitative analysis was conducted by 3 independent blinded observers.

The area of collagen fibers as a function of their color hue was quantified from tissue sections stained with picrosirius red and imaged with circularly polarized light microscopy (200X magnification). The color hue corresponds to relative fiber thickness from thin green fibers to increasingly thick yellow, orange, and red fibers. Following a previously published protocol,[28,29] a custom algorithm was constructed with Matlab software (The Mathworks, Natick, MA) that: (1) cropped each image to only connective tissue directly between mesh fibers removing all subcutaneous connective and underlying muscle tissue; (2) transformed each image from the RGB to the HSV color model; (3) separated each color component as a function of hue (red 2–9 and 230–256, orange 10–38, yellow 39–51, green 52–128); (4) applied a threshold to remove noise from an average of a global threshold using Otsu's method (intensity value of 50/256); and (5) expressed the collagen content for each color component as a percentage of the area of each image.

The infiltrating cell population both adjacent to and in the space between mesh fibers was characterized for expression of the monocyte/macrophage marker CD68. Tissue sections were deparaffinized, subjected to epitope retrieval in 10 mM citrate (pH = 6) at 95°C for 20 minutes, blocked with 1% bovine serum albumin/10% horse serum for 1 hour at room temperature, and labeled with a mouse anti-rat CD68 primary antibody (1:100, clone ED1, MCA341R, AbD Serotec, Raleigh, NC) diluted in 1% bovine serum albumin overnight at 4°C. Endogenous peroxidase activity was quenched with 0.3% (v/v) hydrogen peroxide in distilled water for 15 minutes at room temperature, and then incubated in a HRP conjugated goat anti-mouse secondary antibody (1:200, Vector, Burlingame, CA) diluted in 1% bovine serum albumin for 1 hour at room temperature. Staining developed with the addition of a diaminobenzadine substrate (DAB peroxidase substrate kit, SK4100, Vector) for approximately 6 minutes followed by counterstaining with hematoxylin, dehydration, and coverslipping.

2.6. *Ex vivo* mesh biaxial mechanical properties

The passive biaxial mechanical properties were characterized for the various mesh materials prior to implantation (n=3), and after 35 days for the mesh-tissue explants, unrepaired defect controls (n=8), and the uninjured native abdominal wall (n=5). Immediately following explanation, samples were placed in Ringer's solution supplemented with 0.5 mM verapamil (Sigma) chilled on ice for at least 1 hour prior to testing. The mesh-tissue explants were trimmed to 1.5 cm × 1.5 cm centered over the partial thickness defect region where tissue thickness was measured with a caliper for use in biaxial testing. Biaxial mechanical testing applies a load to a sample along two perpendicular axes simultaneously compared to a

Author Manuscript Author Manuscript Author Manuscript Author Manuscript

uniaxial test were only one axis is loaded. A detailed description of the testing device (Figure 2A) and methods used for planar biaxial testing has been previously reported.[30] Samples were affixed to 250 g load cells (Model 31, Honeywell, Columbus, OH) with two loops of suture attached to each side with four hooks, and deformation was measured from a four marker array centered on the ventral surface after the removal of excess loose connective tissue (Figure 2B). Samples were tested in a Ringers saline solution at room temperature under a equibiaxial stress protocol from a 0.5 g tare load to 85 kPa after 10 cycles of preconditioning with a cycle time of 30 s. All data was referenced to the post-preconditioned free-float state. The maximum strain for each sample was then defined as the strain at the maximum tested stress of 85 kPa.

Each mesh device was tested prior to implantation using a modified biaxial protocol. The edges of the porous mesh samples were heat sealed with polypropylene strips to create a uniform edge for hook attachment. The samples were then formed into a cross-hair shape with each heat sealed edge decoupled from neighboring edges to minimize the boundary condition effect.[31] The center of each sample measured approximately 1.5 cm × 1.5 cm, with an additional 0.25 cm heat sealed edge where hooks were attached (Figure 2C). Adding conventional strain markers, as was done for the tissue samples, would have introduced a non-trivial constraint on the mesh fiber deformation and kinematics, and therefore, strain was defined as total motor displacement over initial sample length. The initial reference state was defined where no slack remained in the suture line. This slack, which would contribute to a false strain measurement, was removed with a 2.5 g tare load. The pre-implant mesh devices do not have a uniform thickness so the load was normalized by sample width to calculate tension, rather than thickness used to calculate stress. Samples were tested under a biaxial and uniaxial load (n=3) after preconditioning to a maximum tension of 100 N/m, which was approximately the tension applied to the mesh-tissue explants using a 85 kPa stress protocol. Maximum strain for the pre-implant mesh devices was defined as the strain at this maximum tension.

2.7. Statistical analysis

The histologic response to mesh materials was compared within time points using a one-way analysis of variance (ANOVA) and Tukey post-hoc analysis to determine significance (p-value < 0.05) with SPSS software (IBM SPSS Statistics, IBM, Armonk, NY). Each histologic remodeling criterion was analyzed independently from the mean values of 3 blinded observers, and this mean value for each image was used for statistical analysis. The biaxial mechanics stress vs. strain and tension vs. strain curves were averaged after a three point linear interpolation at representative stress or tension values with MATLAB software (Mathworks Inc., Natick, MA). A one-way ANOVA and post-hoc Tukey analysis was also used to (significance as p-value < 0.05) to compare maximum strain values All histologic scoring and mechanical analysis values are reported as the mean ± standard error of the mean.

Author Manuscript Author Manuscript Author Manuscript Author Manuscript

3. Results

3.1. Mesh macroscopic appearance and scanning electron microscopy

The heavy-weight BARD™ Mesh possessed a greater fiber density per area (corresponding to smaller pore size) than both light-weight meshes, ULTRAPRO™ and the BARD™ Soft Mesh, as shown both macroscopically (Figure 3A–D) and with scanning electron microscopy (Figure 3E–L). The ECM coating completely covered and adhered to the BARD™ Mesh fibers and knots. The ECM coating was also continuous between mesh fibers and across the pores as a thin coating layer, which remained adherent to the mesh after a 24 hour wash in PBS at 37 °C (Figure 3B, F, J). The BARD™ Soft Mesh had the largest pore size, which was reinforced by 2 small fibers running in parallel across each pore (Figure 3G), and along with ULTRAPRO™ (Figure 3K, L) had larger knots than BARD™ Mesh (Figure 3I).

3.2. Mesh *in vivo* implantation and quantitative histologic analysis

The mesh materials were implanted over a partial thickness abdominal wall defect in the rat for 3, 7, 14, and 35 days. There was macroscopic evidence of new host tissue deposition over the implanted mesh fibers as early as 3 days post implantation, and all mesh materials were fully incorporated into the body wall by 35 days (Figure 1C). The white ECM coating was clearly visible after 3 days, but became less defined over time, eventually becoming indistinguishable from the appearance of the non-coated mesh materials. There was no macroscopic evidence of mesh contracture at any of the time points evaluated.

The histologic response to each mesh material was evaluated by blinded observers from H&E stained sections focusing upon the mesh fiber/tissue interface and the new tissue deposition between mesh fibers (Figure 4, Supplemental Figure 1). The cellularity (Figure 5A) and number of foreign body giant cells (Figure 5B) were similar at the 3, 7, and 14 day time points for the uncoated mesh materials regardless of type, and the majority of these cells expressed the monocyte/macrophage surface marker CD68. However, by 35 days, there was an increase in the number of giant cells that had formed around the uncoated BARD™ Mesh compared to the earlier time points. In contrast, there was a negligible inflammatory cell response to the ECM coated mesh fibers until 14 days (Supplementary Figure 1C), at which point the inflammatory response was obvious but markedly reduced compared to the other materials. The histologic characteristics of the newly deposited tissue between mesh fibers varied with device type. The degree of cellularity (Figure 5C) and vascularity (Figure 5D) was similar for the uncoated BARD™ Mesh and the light-weight mesh devices. Although, these metrics were initially reduced for the ECM coated device compared to the heavy- and light-weight devices, all devices were similar by the final time point. The ECM coating (Figure 4C & Supplementary Figure 1C, D, ECM coating enclosed by dotted line) was not fully degraded until after the 14 day time point, after which it was replaced with loose connective tissue (Figure 4D). The amount and fiber size of deposited collagen fibers between mesh fibers was lower for the ECM coated BARD™ Mesh compared to all other mesh devices after 35 days (Figure 6A–D) as shown with polarized light microscopy quantification (Figure 6E). However, the ECM coated mesh initially (3 day time point) had a greater collagen content than the uncoated heavy-weight mesh, which had

Author Manuscript Author Manuscript Author Manuscript Author Manuscript

minimally detectable amounts (Supplementary Figure 2). In general, there was a reduced response to the ECM coated BARD™ Mesh, though these differences were not always statistically significant.

3.3. *Ex vivo* mesh biaxial mechanical properties

All pre-implant mesh devices were stiff and isotropic under an equibiaxial stress protocol with strain less than 5% and no difference between mesh devices (p-value < 0.05) in either axis (Figure 7A). The maximum strain of all pre-implant mesh devices was greater under a uniaxial protocol compared to an equibiaxial protocol. Maximum strain reached 16% for ULTRAPRO™ (Figure 7B), with a visible degree of anisotropy for each mesh. ULTRAPRO™ had the greatest uniaxial maximum strain and anisotropy compared to the biaxal loading protocol (Figure 7C) followed by BARD™ Soft Mesh (the light-weight mesh devices), while the pre-implant heavyweight BARD™ Mesh and ECM coated BARD™ Mesh showed the lowest uniaxial maximum strain.

The equibiaxial stress response of the native abdominal wall exhibited anisotropic behavior with a maximum strain of 14% and 32% in the circumferential and longitudinal direction, respectively (Figure 8A). The explanted unrepaired defect control had an isotropic response due to a decrease in compliance in the longitudinal direction compared to the native tissue with a 20% maximum strain. Mesh-tissue explants exhibited anisotropic behavior similar to the native tissue after 35 days, and were more compliant in the longitudinal axis compared to the circumferential axis. However, the maximum strains of all mesh-tissue explants in the circumferential direction were less than both the native and unrepaired defect controls (Figure 8B). The maximum strain in the longitudinal direction was highest for the light-weight mesh ULTRAPRO™ at 18% compared to the heavy-weight uncoated and coated BARD™ Mesh at approximately 7% strain.

4. Discussion

The present study provides a detailed temporo-spatial histologic evaluation and comparison of an ECM coated polypropylene mesh with uncoated and light-weight counterparts. The results clearly show the mitigating effect of the ECM coating upon the classic host foreign body response to polypropylene mesh material. This study also presents a detailed biaxial mechanical evaluation of mesh materials embedded within the abdominal wall tissue after 35 days.

Most surgical mesh devices used for ventral hernia repair are composed of synthetic materials with robust mechanical strength, and are typically incorporated quickly into the host tissue.[3–7,9] While these mesh materials provide more than enough strength to prevent hernia recurrence, such devices are associated with non-trivial complications including adhesion, infection, fistula formation, and contraction.[9–11,32,33] Additionally, the innate immune response to the synthetic materials is classically a chronic pro-inflammatory foreign body reaction that promotes fibrotic encapsulation. This fibrotic encapsulation is associated with long-term patient discomfort, which can lead to revision surgery and surgical mesh removal.[9,34] The intensity of the inflammatory response to an implanted mesh may be linked

Author Manuscript Author Manuscript Author Manuscript Author Manuscript

to the degree of tissue ingrowth and scar formation, and modulation of this response can have marked downstream effects.[35]

Numerous design modifications of synthetic surgical mesh materials have been investigated to minimize the clinical complications mentioned above. Changing the mesh architecture to a large pore sized, “light-weight” configuration was shown to be effective for reducing fibrotic mesh encapsulation. The reduction in fibrosis is speculated to be due to the prevention of a continuous scar tissue plane bridging the space between mesh fibers and thus an increase in compliance and prevention of contracture. While the inflammatory response to individual fibers of a light-weight material remains the same, there are fewer exposed fibers per unit area and a cumulative decrease in fibrous tissue deposition.[3,12–14] The smaller pored heavy-weight architecture exposes the recipient to a greater amount and density of foreign body response eliciting material, which presents a challenge to modulate the host response.

Recently, mesh coatings have been investigated to directly modify the host response to the base mesh material. The most commonly evaluated mesh coatings involve prophylactic antimicrobials[36,37] and anti-adhesion films.[38–44] Mesh coatings have also been developed to act as delivery vehicles for therapeutic agents such as immunomodulatory drugs that aim to attenuate the inflammatory response and the resulting downstream fibrosis.[35,45,46] The composition of these coatings varies from synthetic materials including polymers and metal films,[39,47,48] to biologic materials. Biologic mesh coatings include purified collagen,[40] gelatin,[35] hyaluronic acid,[42–44] chitosan,[38] cellulose,[16,39,43] and fatty acids.[39,43] Several of these biologic coating materials are isolated from ECM but in highly purified forms rather than the complex mixture found in the native ECM microenvironment.

Surgical mesh materials composed of allogeneic or xenogeneic extracellular matrix and are capable of facilitating a constructive host remodeling response that contrasts the dense scar tissue deposition in the response to synthetic mesh materials.[19,24] Such devices are typically manufactured by decellularization of various tissues. There are numerous commercially available tissue derived ECM mesh materials used for hernia repair, including dermis, small intestinal submucosa, and pericardium.[21,23,49] ECM devices consist of a complex architecture and biochemical composition, and include a variety of collagenous proteins, glycosaminoglycans, and growth factors that are found in the native matrix of the source tissue.[24] Typically, non-crosslinked ECM devices are rapidly infiltrated by host cells after *in vivo* placement, degraded, and replaced with site appropriate host tissue.[20] ECM mesh materials used for hernia repair have also shown positive remodeling qualities with minimal post-operative pain and long-term complications compared to polypropylene mesh.[15,19] There are several proposed mechanisms by which ECM materials affect the host response, including the release of biologically active matrix fragments during degradation[50,51] and modulation of the innate immune response towards an anti-inflammatory phenotype.[27,49,52] Though not previously utilized in the context of hernia repair, hydrogels composed of ECM degradation products have been characterized and shown to promote a constructive remodeling response *in vivo* further suggesting that ECM fragments may directly affect the default injury response.[27,50,53] Although surgical mesh devices composed of ECM facilitate a favorable host tissue response, such biologic materials typically lack the mechanical

Author Manuscript Author Manuscript Author Manuscript Author Manuscript

strength that is desired and characteristic of synthetic materials.[21–23] The goal of the present study was to combine the advantageous remodeling response of a hydrogel form of ECM with the signature mechanical strength of a polypropylene mesh.

The ECM hydrogel coating was effective at markedly altering the histologic host remodeling response. The uncoated polypropylene mesh evoked a classic foreign body response, with a rapid accumulation of mononuclear cells and foreign body giant cells around mesh fibers, whereas the ECM coated mesh attenuated the inflammatory response. During the acute phase after implantation relatively few host cells contacted the polypropylene mesh through the ECM coating, preventing the characteristic accumulation of CD68+ cells immediately adjacent to the mesh fibers. This effect persisted until at least 35 days, by which time the coating had degraded and been replaced by loose collagenous connective tissue. Direct cell contact with synthetic polymers has been shown to activate fibroblasts and macrophages *in vitro* to release pro-inflammatory cytokines that direct new tissue deposition and remodeling including TGF-β, IL-6, and matrix metalloproteinases.[32,54,55] Thus the ECM coating may shield the mesh device from acute host inflammatory activation, promote filling of the pores with loose connective tissue, and facilitate the immunomodulatory effects described for implanted ECM scaffolds.[49,52]

The light-weight mesh devices elicited a pronounced inflammatory response adjacent to the mesh fibers, indicating that the host response to the base polypropylene material was not affected by mesh pore size. Tissue ingrowth and remodeling between mesh fibers (i.e. the pores) were also affected by an ECM coating. The initial cellular infiltrate into mesh pore regions was reduced for ECM coated meshes, though this effect had diminished by 35 days. The pores in the ECM coated mesh materials had filled with loose connective tissue after 35 days rather than the dense, large fiber collagenous tissue noted in the uncoated mesh material pores as shown by polarized light microscopy. The initial collagen content in the ECM coated mesh was likely the coating material itself, and subsequent time points represent a combination of ECM degradation and new host collagen deposition. The high collagen density between mesh fibers of the lightweight mesh devices was localized to a thin band of mature collagen compared to the thicker bands found in the heavy-weight mesh. Though the ECM coated mesh had a reduced collagen density, it was fully incorporated into the adjacent abdominal wall as evident from full mesh adherence via macroscopic and histologic observation.

The biaxial mechanical testing provides insights into the mechanical properties of abdominal wall tissue following repair with a surgical mesh material. The creation of a partial thickness defect is sufficient to induce an isotropic response. The anisotropy of the mesh-tissue explant is similar to that seen in the native body wall control, but is also seemingly counterintuitive since the equibiaxial characterization of all mesh devices prior to implantation indicates a stiff isotropic response. Detailed examination of the mesh devices prior to implantation showed that there was a strong degree of axial coupling for the lightweight meshes. There were larger maximum strain values and pronounced anisotropy for all devices under uniaxial protocols compared to the stiff isotropic response in a biaxial protocol. However, none of the explanted mesh devices reached strain values observed in the native abdominal wall, though the lightweight mesh devices did have a greater

Author Manuscript Author Manuscript Author Manuscript Author Manuscript

maximum strain compared to the heavy-weight mesh devices. Only ULTRAPRO™ contained a degradable mesh fiber component that may change the mesh properties during remodeling. Therefore, neither the maximum equibiaxial strain of the pre-implant mesh device nor of the injured tissue in isolation predicts the strain nor the degree of anisotropy found in the mesh-tissue explants. These findings suggest complex mechanical interactions between mesh devices, underlying host tissue, and newly deposited connective tissue. Although the histologic connective tissue density was reduced for ECM coated mesh devices, this did not translate to a reduction in the mechanical properties or separation from the underlying abdominal wall during testing. The robust mechanical properties of the base heavyweight mesh may dominate the mesh mechanical properties in this model.

Further investigation is required to determine if the anisotropic response of the mesh-tissue explant under biaxial load is due to oriented tissue deposition or changes localized mesh contraction (i.e. small changes in mesh fiber orientation without contraction of the bulk mesh device). Some of the differences between the heavy- and light-weight devices may also be due to stress-shielding effects of the heavy-weight mesh. Stress shielding may occur when loads are not effectively transferred to the newly deposited tissue and thereby negatively affecting remodeling.[56] The light-weight mesh devices, which are more compliant under uniaxial loads, may not induce this stress shielding effect.

To the authors' knowledge this is the first time the planar biaxial mechanics of mesh devices prior to implantation and mesh-tissue composite explants have been characterized. The most frequently used mechanical test for mesh devices prior to implantation and for mesh-tissue composite explants is a uniaxial test to failure which is taken to supraphysiologic loads and does not replicate the complex multi-axial boundary conditions seen in repairs.[4,6,8] While the anisotropy can be captured if the samples are tested along both axes, the observed complex axial coupling, as shown here, cannot be replicated.

Light-weight mesh devices are widely accepted for hernia repair, in part because of the decreased amount of foreign material per unit area available to induce a foreign body response. The present study shows that an ECM coating mitigates the default foreign body response to polypropylene mesh fibers in a heavy-weight mesh material. It is reasonable to expect that this mitigating effect will also apply to light-weight mesh fibers, though this has yet to be investigated. The ability of an ECM coating to reduce the inflammatory response and the associated foreign body reaction to polypropylene mesh would logically be associated with a decrease in the complications associated with such materials including dense fibrotic encapsulation, mesh contracture, and patient discomfort.[9–11] If such a favorable change in the classic tissue response process is true, then applications such as pelvic floor repair and breast reconstruction would benefit greatly. The methodology described herein has the potential to be applied to other mesh configurations and mesh materials. A limitation of the present study was the relatively short duration of 35 days. Continued remodeling within and surrounding the mesh material and the long term effect following the complete degradation of the ECM coating must be evaluated.

Author Manuscript Author Manuscript Author Manuscript Author Manuscript

5. Conclusions

A method to successfully coat a synthetic heavy-weight polypropylene hernia mesh with an ECM hydrogel is described. This ECM coating effectively altered the default host response to the base polypropylene mesh by delaying and reducing the accumulation of pro-inflammatory foreign body giant cells. The new host tissue deposition was altered such that the result after 35 days in a rodent model was more similar to a light-weight mesh than the base heavy-weight mesh. However, the differences in remodeling of an ECM coated mesh did not translate to a reduction in biaxial mechanical response. An ECM coating can favorably alter at least the short term tissue remodeling within and surrounding an implanted polypropylene heavy-weight mesh.

Supplementary Material

Refer to Web version on PubMed Central for supplementary material.

Acknowledgments

Partial funding for this study was provided by C.R. Bard, Inc. Matthew Wolf was partially supported by the NIH-NHLBI training grant (T32-HL76124-6) entitled “Cardiovascular Bioengineering Training Program” through the University of Pittsburgh Department of Bioengineering. Christopher Medberry and Ricardo Londono were partially supported by the NIH-NHLBI training grant (T32-EB001026) entitled “Cellular Approaches to Tissue Engineering and Regeneration.” Christopher Carruthers was partially supported by the National Science Foundation (NSF) Graduate Research Fellowship. Olivia Burnsed was supported by the National Science Foundation under Grant No. (1004836). Any opinions, findings, and conclusions or recommendations expressed in this material are those of the author(s) and do not necessarily reflect the views of the National Science Foundation. The authors would like to thank Deanna Rhoads and the McGowan Histology Center for histologic section preparation and the center for Biologic Imaging at the University of Pittsburgh for access to imaging facilities. The authors would also like to thank Janet Reing, Hongbin Jiang, Sydney Gibson, Dr. Kristen Jones, Dr. Rouzbeh Amini, and Jenna Dziki for their assistance with animal care and manuscript preparation.

References

1. Usher FC. Hernia Repair with Knitted Polypropylene Mesh. Surg Gynecol Obstet. 1963; 117:239–40. [PubMed: 14048019]
2. George CD, Ellis H. The results of incisional hernia repair: a twelve year review. Ann R Coll Surg Engl. 1986; 68(4):185–7. [PubMed: 3789602]
3. Cobb WS, Kercher KW, Heniford BT. The argument for lightweight polypropylene mesh in hernia repair. Surg Innov. 2005; 12(1):63–9. [PubMed: 15846448]
4. Feola A, Barone W, Moalli P, Abramowitch S. Characterizing the ex vivo textile and structural properties of synthetic prolapse mesh products. Int Urogynecol J. 2012
5. Klosterhalfen B, Junge K, Klinge U. The lightweight and large porous mesh concept for hernia repair. Expert Rev Med Devices. 2005; 2(1):103–17. [PubMed: 16293033]
6. Hernandez-Gascon B, Pena E, Melero H, Pascual G, Doblare M, Ginebra MP, Bellon JM, Calvo B. Mechanical behaviour of synthetic surgical meshes: finite element simulation of the herniated abdominal wall. Acta Biomater. 2011; 7(11):3905–13. [PubMed: 21763794]
7. Chu CC, Welch L. Characterization of morphologic and mechanical properties of surgical mesh fabrics. J Biomed Mater Res. 1985; 19(8):903–16. [PubMed: 3880350]
8. Ozog Y, Konstantinovic M, Werbrouck E, De Ridder D, Mazza E, Deprest J. Persistence of polypropylene mesh anisotropy after implantation: an experimental study. BJOG. 2011; 118(10): 1180–5. [PubMed: 21668770]
9. Klinge U, Klosterhalfen B, Muller M, Schumpelick V. Foreign body reaction to meshes used for the repair of abdominal wall hernias. Eur J Surg. 1999; 165(7):665–73. [PubMed: 10452261]

Author Manuscript Author Manuscript Author Manuscript Author Manuscript

10. Leber GE, Garb JL, Alexander AI, Reed WP. Long-term complications associated with prosthetic repair of incisional hernias. Arch Surg. 1998; 133(4):378–82. [PubMed: 9565117]
11. Brown CN, Finch JG. Which mesh for hernia repair? Ann R Coll Surg Engl. 2010; 92(4):272–8. [PubMed: 20501011]
12. Hollinsky C, Sandberg S, Koch T, Seidler S. Biomechanical properties of lightweight versus heavyweight meshes for laparoscopic inguinal hernia repair and their impact on recurrence rates. Surg Endosc. 2008; 22(12):2679–85. [PubMed: 18443869]
13. Weyhe D, Schmitz I, Belyaev O, Grabs R, Muller KM, Uhl W, Zumtobel V. Experimental comparison of monofile light and heavy polypropylene meshes: less weight does not mean less biological response. World J Surg. 2006; 30(8):1586–91. [PubMed: 16855805]
14. Conze J, Rosch R, Klinge U, Weiss C, Anurov M, Titkowa S, Oettinger A, Schumpelick V. Polypropylene in the intra-abdominal position: influence of pore size and surface area. Hernia. 2004; 8(4):365–72. [PubMed: 15309687]
15. Ansaloni L, Catena F, Coccolini F, Gazzotti F, D'Alessandro L, Pinna AD. Inguinal hernia repair with porcine small intestine submucosa: 3-year follow-up results of a randomized controlled trial of Lichtenstein's repair with polypropylene mesh versus Surgisis Inguinal Hernia Matrix. Am J Surg. 2009; 198(3):303–12. [PubMed: 19285658]
16. Medberry CJ, Tottey S, Jiang H, Johnson SA, Badylak SF. Resistance to Infection of Five Different Materials in a Rat Body Wall Model. J Surg Res. 2010
17. Holton LH 3rd, Chung T, Silverman RP, Haerian H, Goldberg NH, Burrows WM, Gobin A, Butler CE. Comparison of acellular dermal matrix and synthetic mesh for lateral chest wall reconstruction in a rabbit model. Plast Reconstr Surg. 2007; 119(4):1238–46. [PubMed: 17496596]
18. Valentin JE, Turner NJ, Gilbert TW, Badylak SF. Functional skeletal muscle formation with a biologic scaffold. Biomaterials. 2010; 31(29):7475–84. [PubMed: 20638716]
19. Hiles M, Record Ritchie RD, Altizer AM. Are biologic grafts effective for hernia repair?: a systematic review of the literature. Surg Innov. 2009; 16(1):26–37. [PubMed: 19223383]
20. Valentin JE, Stewart-Akers AM, Gilbert TW, Badylak SF. Macrophage participation in the degradation and remodeling of extracellular matrix scaffolds. Tissue Eng Part A. 2009; 15(7): 1687–94. [PubMed: 19125644]
21. Deeken CR, Melman L, Jenkins ED, Greco SC, Frisella MM, Matthews BD. Histologic and biomechanical evaluation of crosslinked and non-crosslinked biologic meshes in a porcine model of ventral incisional hernia repair. J Am Coll Surg. 2011; 212(5):880–8. [PubMed: 21435917]
22. Bellows CF, Wheatley BM, Moroz K, Rosales SC, Morici LA. The effect of bacterial infection on the biomechanical properties of biological mesh in a rat model. PLoS One. 2011; 6(6):e21228. [PubMed: 21698179]
23. Zhang J, Wang GY, Xiao YP, Fan LY, Wang Q. The biomechanical behavior and host response to porcine-derived small intestine submucosa, pericardium and dermal matrix acellular grafts in a rat abdominal defect model. Biomaterials. 2011; 32(29):7086–95. [PubMed: 21741703]
24. Badylak SF, Freytes DO, Gilbert TW. Extracellular matrix as a biological scaffold material: Structure and function. Acta Biomater. 2009; 5(1):1–13. [PubMed: 18938117]
25. Reing JE, Brown BN, Daly KA, Freund JM, Gilbert TW, Hsiong SX, Huber A, Kullas KE, Tottey S, Wolf MT, et al. The effects of processing methods upon mechanical and biologic properties of porcine dermal extracellular matrix scaffolds. Biomaterials. 2010; 31(33):8626–33. [PubMed: 20728934]
26. Freytes DO, Martin J, Velankar SS, Lee AS, Badylak SF. Preparation and rheological characterization of a gel form of the porcine urinary bladder matrix. Biomaterials. 2008; 29(11): 1630–7. [PubMed: 18201760]
27. Wolf MT, Daly KA, Brennan-Pierce EP, Johnson SA, Carruthers CA, D'Amore A, Nagarkar SP, Velankar SS, Badylak SF. A hydrogel derived from decellularized dermal extracellular matrix. Biomaterials. 2012; 33(29):7028–38. [PubMed: 22789723]
28. Rich L, Whittaker P. Collagen and picrosirius red staining: a polarized light assesment of fibrillar hue and spatial distribution. Braz J morphol Sci. 2005; 22(2):97–104.
29. Nadkarni SK, Pierce MC, Park BH, de Boer JF, Whittaker P, Bouma BE, Bressner JE, Halpern E, Houser SL, Tearney GJ. Measurement of collagen and smooth muscle cell content in

Author Manuscript Author Manuscript Author Manuscript Author Manuscript

atherosclerotic plaques using polarization-sensitive optical coherence tomography. J Am Coll Cardiol. 2007; 49(13):1474–81. [PubMed: 17397678]

30. Billiar KL, Sacks MS. Biaxial mechanical properties of the natural and glutaraldehyde treated aortic valve cusp--Part I: Experimental results. J Biomech Eng. 2000; 122(1):23–30. [PubMed: 10790826]
31. Sun W, Sacks MS, Scott MJ. Effects of boundary conditions on the estimation of the planar biaxial mechanical properties of soft tissues. J Biomech Eng. 2005; 127(4):709–15. [PubMed: 16121542]
32. Di Vita G, D'Agostino P, Patti R, Arcara M, Caruso G, Davi V, Cillari E. Acute inflammatory response after inguinal and incisional hernia repair with implantation of polypropylene mesh of different size. Langenbecks Arch Surg. 2005; 390(4):306–11. [PubMed: 15690201]
33. Garcia-Urena MA, Vega Ruiz V, Diaz Godoy A, Baez Perea JM, Marin Gomez LM, Carnero Hernandez FJ, Velasco Garcia MA. Differences in polypropylene shrinkage depending on mesh position in an experimental study. Am J Surg. 2007; 193(4):538–42. [PubMed: 17368306]
34. Costello CR, Bachman SL, Ramshaw BJ, Grant SA. Materials characterization of explanted polypropylene hernia meshes. J Biomed Mater Res B Appl Biomater. 2007; 83(1):44–9. [PubMed: 17285608]
35. Brandt CJ, Kammer D, Fiebeler A, Klinge U. Beneficial effects of hydrocortisone or spironolactone coating on foreign body response to mesh biomaterial in a mouse model. J Biomed Mater Res A. 2011; 99(3):335–43. [PubMed: 22021181]
36. Harth KC, Rosen MJ, Thatiparti TR, Jacobs MR, Halaweish I, Bajaksouzian S, Furlan J, von Recum HA. Antibiotic-releasing mesh coating to reduce prosthetic sepsis: an in vivo study. J Surg Res. 2010; 163(2):337–43. [PubMed: 20538302]
37. Engelsman AF, Krom BP, Busscher HJ, van Dam GM, Ploeg RJ, van der Mei HC. Antimicrobial effects of an NO-releasing poly(ethylene vinylacetate) coating on soft-tissue implants in vitro and in a murine model. Acta Biomater. 2009; 5(6):1905–10. [PubMed: 19251498]
38. Altinel Y, Ozturk E, Ozkaya G, Akyildiz EU, Ulcay Y, Ozguc H. The effect of a chitosan coating on the adhesive potential and tensile strength of polypropylene meshes. Hernia. 2012
39. Schreinemacher MH, Emans PJ, Gijbels MJ, Greve JW, Beets GL, Bouvy ND. Degradation of mesh coatings and intraperitoneal adhesion formation in an experimental model. Br J Surg. 2009; 96(3):305–13. [PubMed: 19224521]
40. van't Riet M, Burger JW, Bonthuis F, Jeekel J, Bonjer HJ. Prevention of adhesion formation to polypropylene mesh by collagen coating: a randomized controlled study in a rat model of ventral hernia repair. Surg Endosc. 2004; 18(4):681–5. [PubMed: 15026899]
41. Borrazzo EC, Belmont MF, Boffa D, Fowler DL. Effect of prosthetic material on adhesion formation after laparoscopic ventral hernia repair in a porcine model. Hernia. 2004; 8(2):108–12. [PubMed: 14634842]
42. Fujino K, Kinoshita M, Saitoh A, Yano H, Nishikawa K, Fujie T, Iwaya K, Kakihara M, Takeoka S, Saitoh D, et al. Novel technique of overlaying a poly-L: -lactic acid nanosheet for adhesion prophylaxis and fixation of intraperitoneal onlay polypropylene mesh in a rabbit model. Surg Endosc. 2011; 25(10):3428–36. [PubMed: 21638189]
43. Pierce RA, Perrone JM, Nimeri A, Sexton JA, Walcutt J, Frisella MM, Matthews BD. 120-day comparative analysis of adhesion grade and quantity, mesh contraction, and tissue response to a novel omega-3 fatty acid bioabsorbable barrier macroporous mesh after intraperitoneal placement. Surg Innov. 2009; 16(1):46–54. [PubMed: 19124448]
44. van 't Riet M, de Vos van Steenwijk PJ, Bonthuis F, Marquet RL, Steyerberg EW, Jeekel J, Bonjer HJ. Prevention of adhesion to prosthetic mesh: comparison of different barriers using an incisional hernia model. Ann Surg. 2003; 237(1):123–8. [PubMed: 12496539]
45. Maciver AH, McCall MD, Edgar RL, Thiesen AL, Bigam DL, Churchill TA, Shapiro AM. Sirolimus drug-eluting, hydrogel-impregnated polypropylene mesh reduces intra-abdominal adhesion formation in a mouse model. Surgery. 2011; 150(5):907–15. [PubMed: 21943642]
46. Takaoka R, Hikasa Y, Tabata Y. Vascularization around poly(tetrafluoroethylene) mesh with coating of gelatin hydrogel incorporating basic fibroblast growth factor. J Biomater Sci Polym Ed. 2009; 20(10):1483–94. [PubMed: 19622284]

Author Manuscript Author Manuscript Author Manuscript Author Manuscript

47. Badiou W, Lavigne JP, Bousquet PJ, O'Callaghan D, Mares P, de Tayrac R. In vitro and in vivo assessment of silver-coated polypropylene mesh to prevent infection in a rat model. Int Urogynecol J. 2011; 22(3):265–72. [PubMed: 21107810]

48. Junge K, Rosch R, Klinge U, Saklak M, Klosterhalfen B, Peiper C, Schumpelick V. Titanium coating of a polypropylene mesh for hernia repair: effect on biocompatibilty. Hernia. 2005; 9(2): 115–9. [PubMed: 15583967]

49. Brown BN, Londono R, Tottey S, Zhang L, Kukla KA, Wolf MT, Daly KA, Reing JE, Badylak SF. Macrophage phenotype as a predictor of constructive remodeling following the implantation of biologically derived surgical mesh materials. Acta Biomater. 2012; 8(3):978–87. [PubMed: 22166681]

50. DeQuach JA, Lin JE, Cam C, Hu D, Salvatore MA, Sheikh F, Christman KL. Injectable skeletal muscle matrix hydrogel promotes neovascularization and muscle cell infiltration in a hindlimb ischemia model. Eur Cell Mater. 2012; 23:400–12. discussion 412. [PubMed: 22665162]

51. Agrawal V, Johnson SA, Reing J, Zhang L, Tottey S, Wang G, Hirschi KK, Braunhut S, Gudas LJ, Badylak SF. Epimorphic regeneration approach to tissue replacement in adult mammals. Proc Natl Acad Sci U S A. 2010; 107(8):3351–5. [PubMed: 19966310]

52. Badylak SF, Valentin JE, Ravindra AK, McCabe GP, Stewart-Akers AM. Macrophage phenotype as a determinant of biologic scaffold remodeling. Tissue Eng Part A. 2008; 14(11):1835–42. [PubMed: 18950271]

53. Singelyn JM, Sundaramurthy P, Johnson TD, Schup-Magoffin PJ, Hu DP, Faulk DM, Wang J, Mayle KM, Bartels K, Salvatore M, et al. Catheter-deliverable hydrogel derived from decellularized ventricular extracellular matrix increases endogenous cardiomyocytes and preserves cardiac function post-myocardial infarction. J Am Coll Cardiol. 2012; 59(8):751–63. [PubMed: 22340268]

54. Weyhe D, Belyaev O, Buettner G, Mros K, Mueller C, Meurer K, Papapostolou G, Uhl W. In vitro comparison of three different mesh constructions. ANZ J Surg. 2008; 78(1–2):55–60. [PubMed: 18199207]

55. Weyhe D, Hoffmann P, Belyaev O, Mros K, Muller C, Uhl W, Schmitz F. The role of TGF-beta1 as a determinant of foreign body reaction to alloplastic materials in rat fibroblast cultures: comparison of different commercially available polypropylene meshes for hernia repair. Regul Pept. 2007; 138(1):10–4. [PubMed: 16973225]

56. Muellner T, Kwasny O, Loehnert V, Mallinger R, Unfried G, Schabus R, Plenk H Jr. Light and electron microscopic study of stress-shielding effects on rat patellar tendon. Arch Orthop Trauma Surg. 2001; 121(10):561–5. [PubMed: 11768636]

Author Manuscript Author Manuscript Author Manuscript Author Manuscript

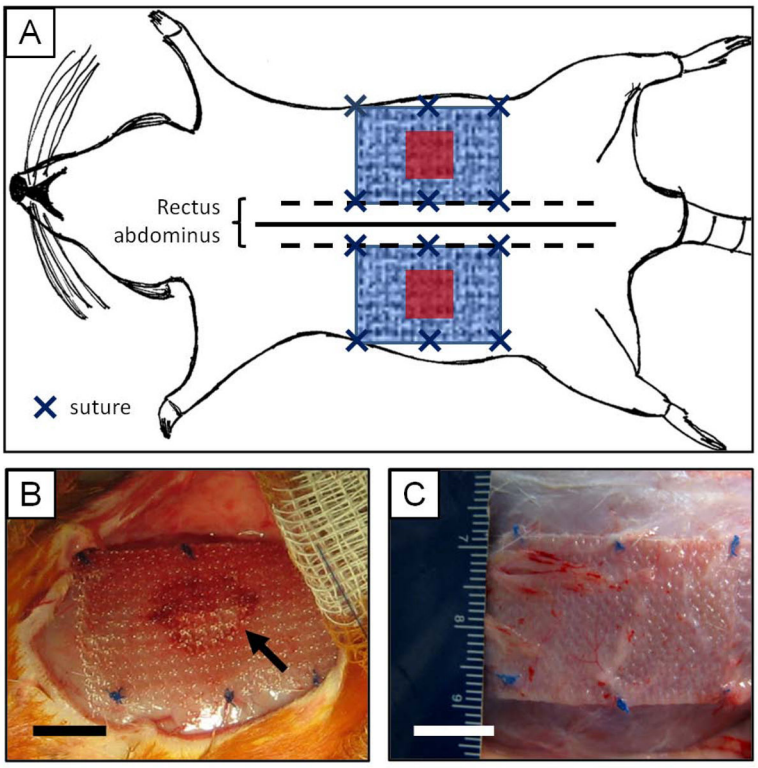

Figure 1.

Surgical model of mesh implantation in the rat. (A) Schematic representation of mesh placement. Two 1 cm × 1 cm partial thickness abdominal wall paramedian defects were created (red squares), and were repaired with 2 cm × 3 cm mesh devices (blue patterned rectangle) using an overlay technique. Each mesh was parallel to the midline (solid line) and bordered the edge of the *rectus abdominus* (dotted line). Mesh devices were fixed to the abdominal using 6 single interrupted sutures (dark blue " "s) along the edge of the mesh. (B) The BARD™ Mesh during the implantation surgery over the partial thickness defect (visible through the mesh pores, arrow) and fixed to the abdominal wall with 6 sutures around the edge of the mesh (blue knots). (C) The BARD™ Mesh *in situ* 35 days post implantation. Scale bar represents 1 cm.

Author Manuscript Author Manuscript Author Manuscript Author Manuscript

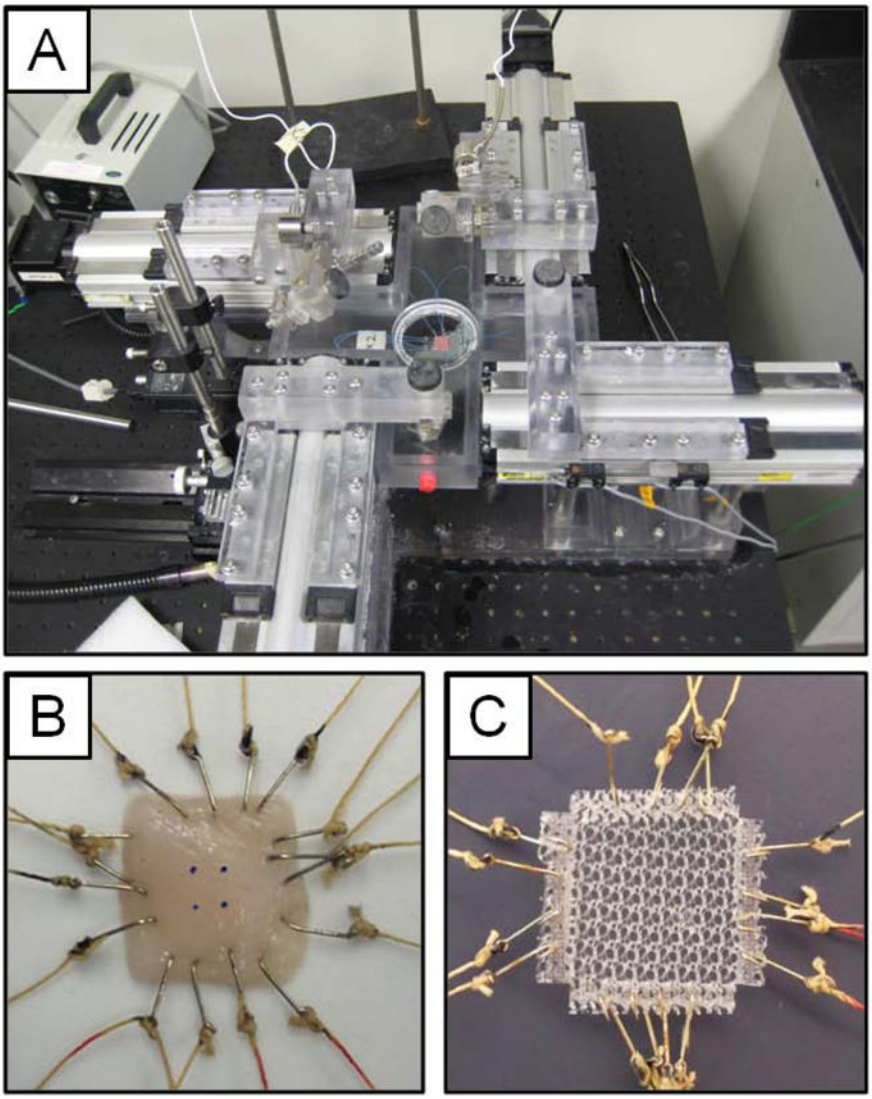

Figure 2.

Planar biaxial mechanical testing system and methods. (A) Planar biaxial testing system shown with a prepared tissue sample. (B) Abdominal wall tissue prepared for biaxial testing. Two sets of looped suture were attached along each edge of tissue samples using hooks to apply force, and a 4 marker array was placed in the center of the sample to track deformation. (C) Pre-implantation mesh sample preparation for biaxial testing. Mesh samples were cut into squares and the edges were heat sealed with strips of polypropylene. Each device was then cut into a cross-hair shape, and two sets of looped suture were attached through the heat sealed edge using hooks.

Author Manuscript Author Manuscript Author Manuscript Author Manuscript

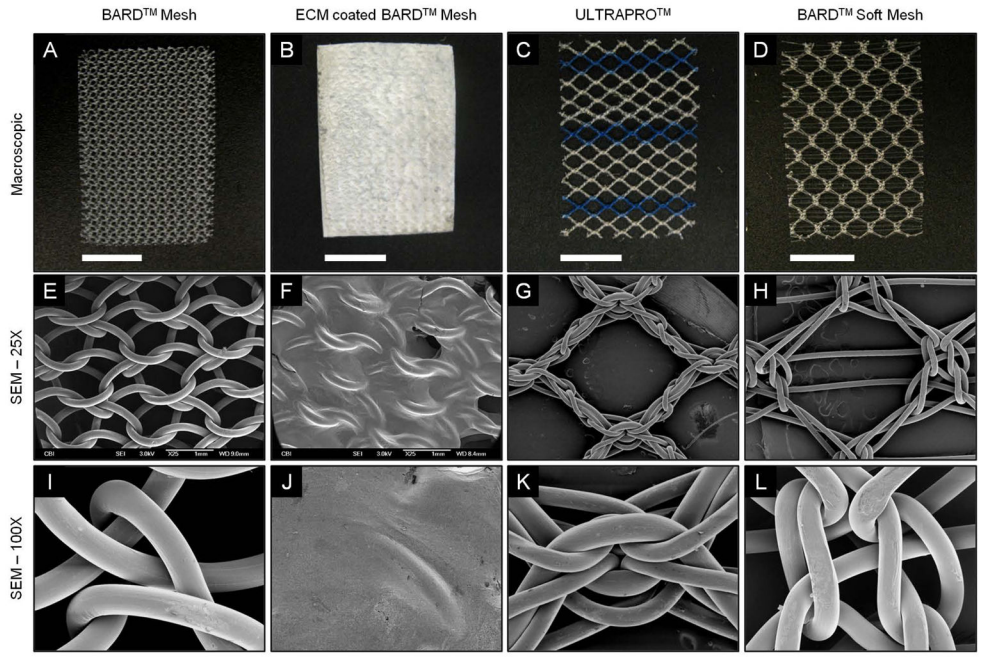

Figure 3.

Macroscopic appearance and scanning electron micrographs of mesh devices. BARD™ Mesh, ECM coated BARD™ Mesh, ULTRAPRO™, and BARD™ Soft Mesh devices were compared macroscopically (top row) and with scanning electron microscopy. Scanning electron micrographs were imaged at 25X magnification (middle row) centered over mesh pores and at 100X magnification (bottom row) centered over mesh knots. Scale bars in macroscopic images represent 1 cm.

Author Manuscript Author Manuscript Author Manuscript Author Manuscript

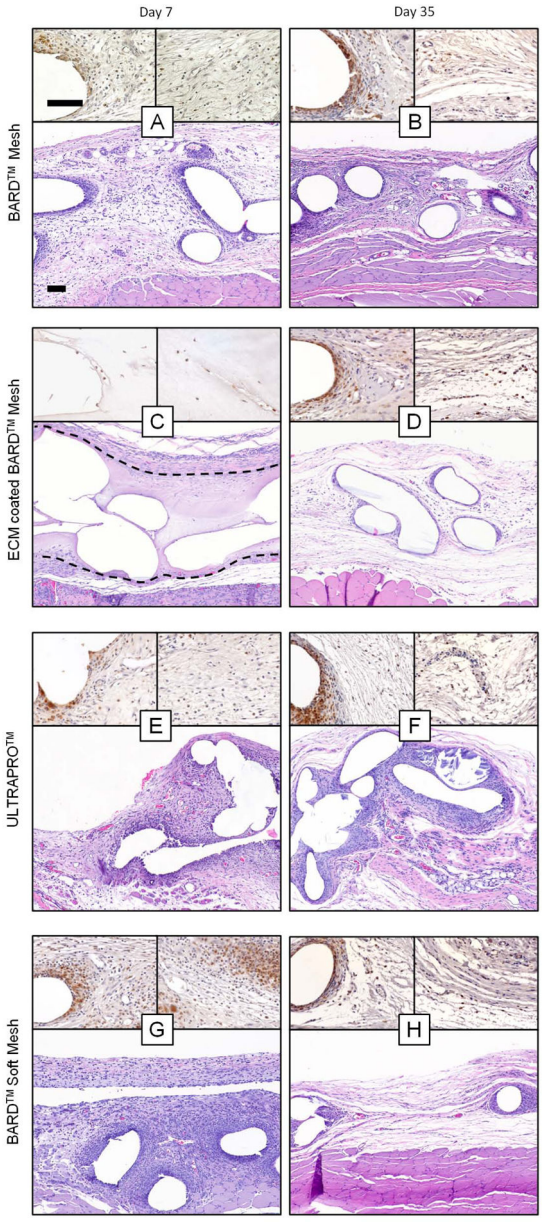

Figure 4.

Histologic appearance of mesh devices after 7 and 35 days of *in vivo* implantation. Representative H&E stained histologic cross sections of each mesh/time point were imaged at 100X magnification (bottom of each figure panel). Two 400X magnification images immunolabeled for the macrophage marker CD68 (brown) were focused on the area adjacent to mesh fibers (top left of each panel) and the area between mesh fibers (top right of each panel). Dotted line in C encloses the ECM coating surrounding the mesh fibers. Scale bars represents 100 μm.

Author Manuscript Author Manuscript Author Manuscript Author Manuscript

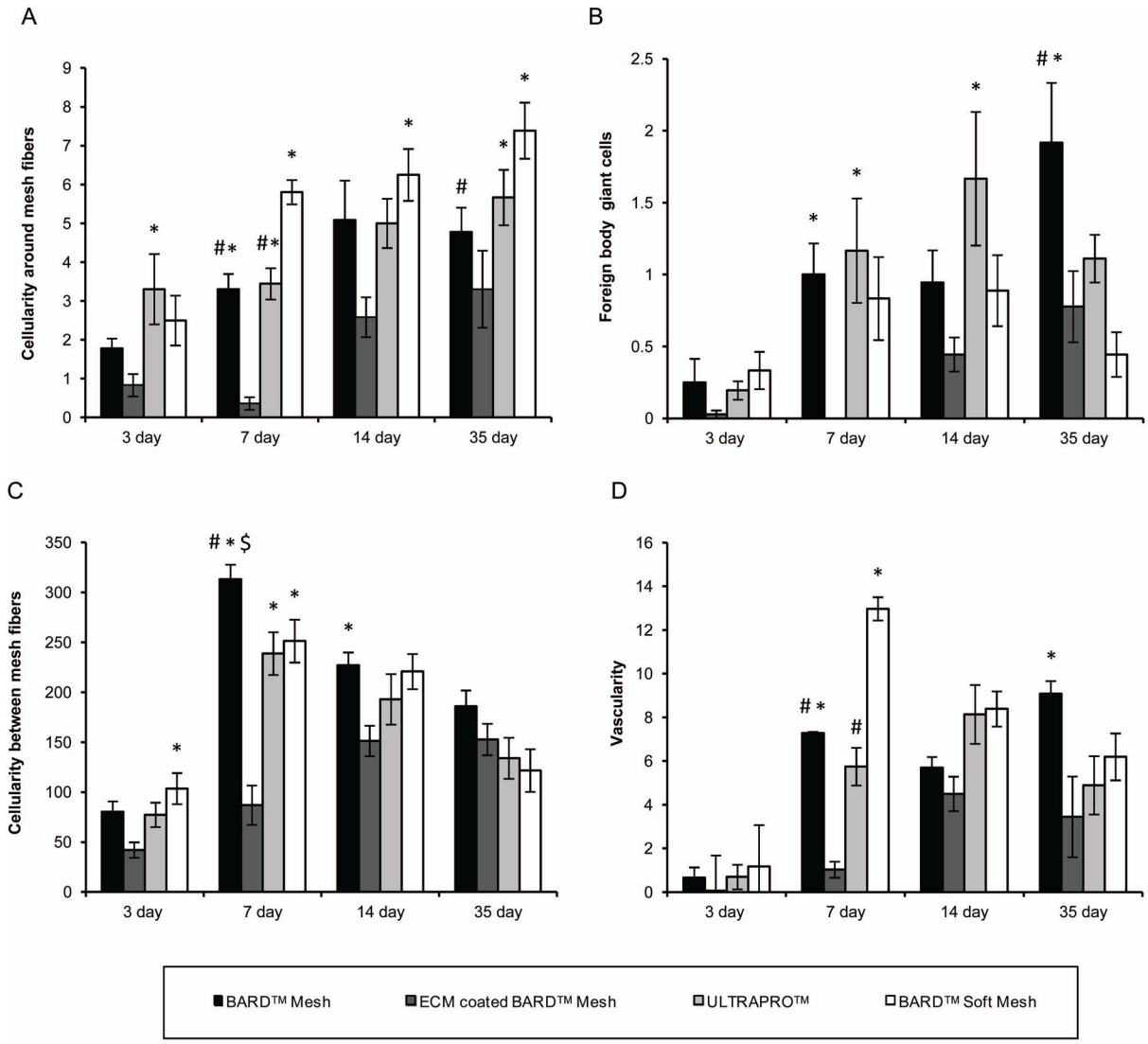

Figure 5.

Histomorphometric analysis of the histologic inflammatory response to mesh fibers and tissue remodeling in the area between mesh fibers from H&E stained histologic cross sections after 3, 7, 14, and 35 days post implantation. (A) The mesh fiber cellularity and (B) number of foreign body giant cells for each device were counted to characterize the inflammatory response to mesh fibers. Tissue remodeling between mesh fibers was analyzed as the (C) number of mononuclear cells and (D) number of blood vessels. Significant differences (p-value < 0.05) between devices within each time point are denoted: (*) as different from the ECM coated BARD™ Mesh, ($) as different from ULTRAPRO™, and (#) as different from BARD™ Soft Mesh.

Author Manuscript Author Manuscript Author Manuscript Author Manuscript

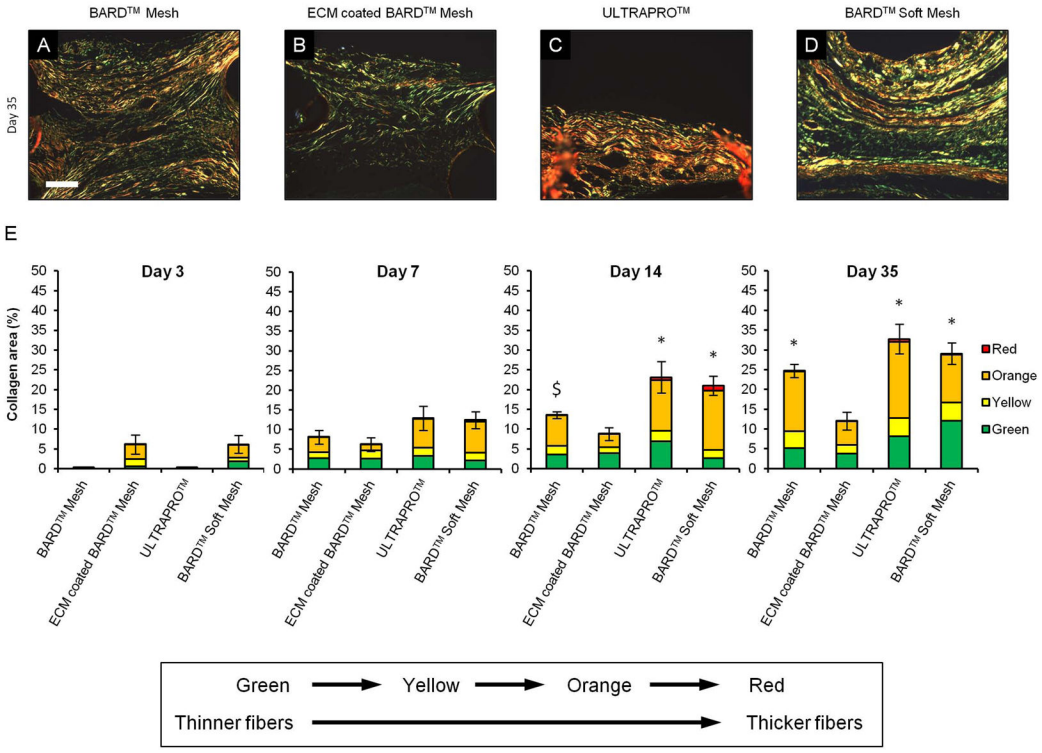

Figure 6.

Picrosirius red staining and quantification of collagen area between mesh fibers using polarized light microscopy. (A–D) Collagen fibers between the mesh fibers of each device after 35 days. The color hue of the fibers represents the relative collagen thicknesses: (in order of thinnest to thickest) green, yellow, orange, and red. (E) Quantification of the total area and proportion of collagen (defined by color hue) in each mesh after 3, 7, 14, and 35 days. Significant differences (p-value < 0.05) in total collagen content between devices within each time point are denoted: (*) as different from the ECM coated BARD™ Mesh, ($) as different from ULTRAPRO™, and (#) as different from BARD™ Soft Mesh. Scale bar represents 100 μm.

Author Manuscript Author Manuscript Author Manuscript Author Manuscript

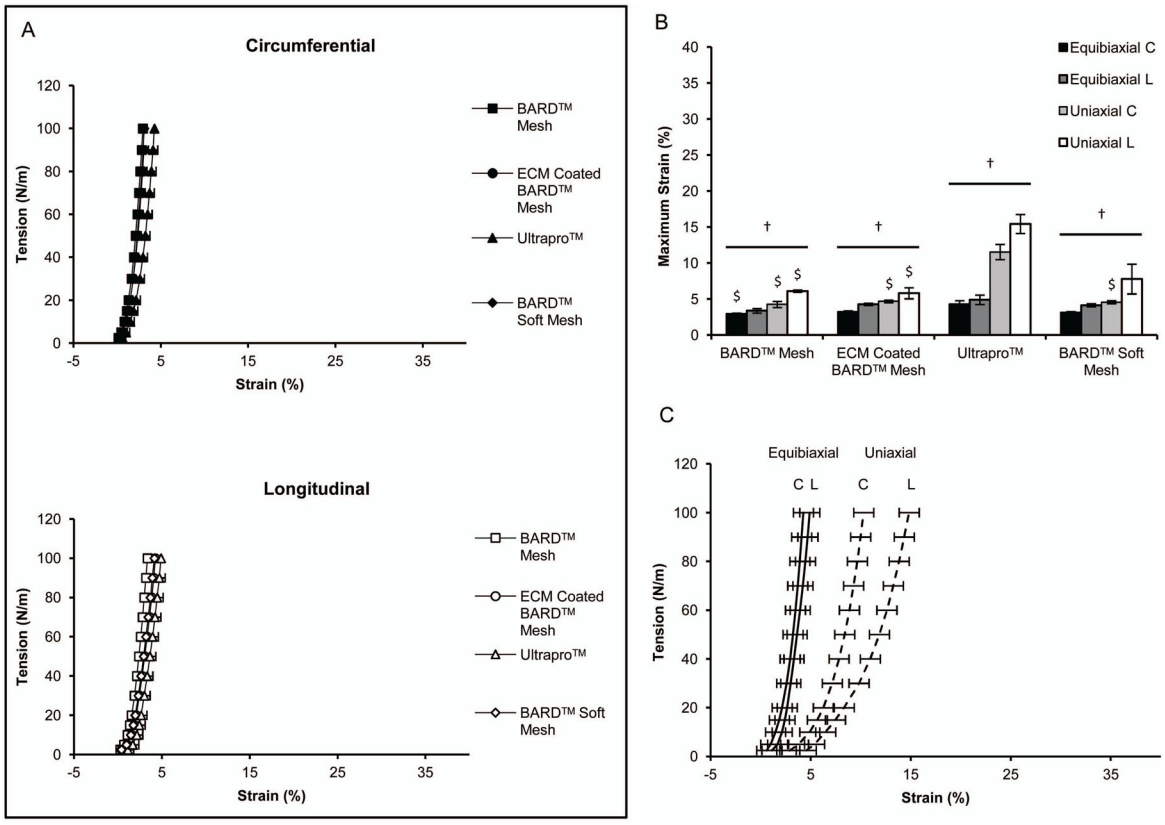

Figure 7.

Pre-implantation mesh mechanical characterization. (A) The equibiaxial tension response of mesh devices was characterized along the circumferential-C and longitudinal-L axes. (B) The maximum strain defined at a tension of 100 N/m for both equibiaxial and uniaxial protocols. (C) Comparison of biaxial and uniaxial tension protocols for the ULTRAPRO™ mesh along the circumferential-C and longitudinal-L axes. Significant differences (p-value < 0.05) between ULTRAPRO™ and each material within the same axis and testing protocol are denoted with ($). Significant differences between equibiaxial and uniaxial testing protocols for each device are denoted with (†).

Author Manuscript Author Manuscript Author Manuscript Author Manuscript

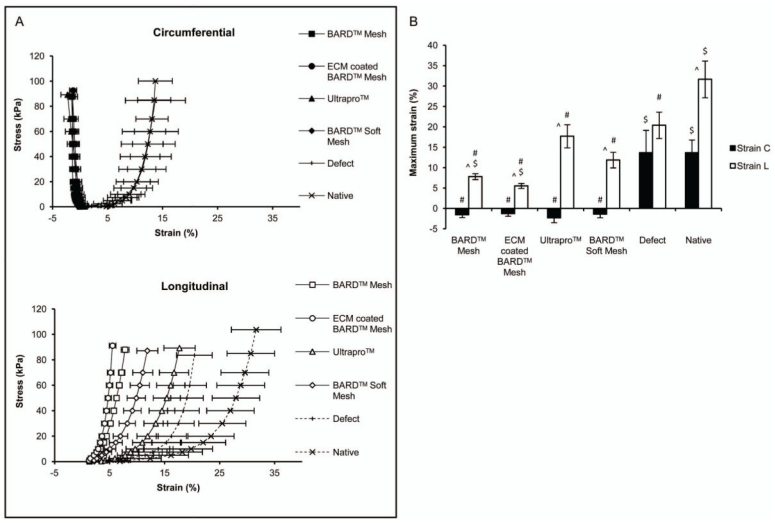

Figure 8.

Mesh explants equibiaxial mechanical characterization after 35 days. (A) The equibiaxial stress response of the explanted mesh devices were characterized along the circumferential and longitudinal axes. (B) The maximum strain defined at a stress of 85 kPa for both circumferential-C and longitudinal-L axes. Significant differences (p-value < 0.05) between the circumferential and longitudinal axes of the same sample are denoted with (^). Significant differences between samples in each axis are denoted as the following: ($) as different from ULTRAPRO™ and (#) as different from the uninjured native tissue.

Author Manuscript

Author Manuscript

Author Manuscript

Author Manuscript

Table 1

Summary of quantitative histomorphometric analysis categories. The host response to implanted mesh devices was evaluated according to criteria that evaluated the inflammatory response to mesh fibers (cellularity and foreign body giant cell formation) and the remodeling characteristics of the area between mesh fibers (celluarity, vascularity, and collagenous connective tissue deposition).

Region	Category	Description of quantitative analysis
Mesh fiber/tissue interface	Cellularity	Number of cell layers of dense cellular accumulation immediately adjacent to fibers per FOV
	Foreign body giant cells	Number of foreign body giant cells per FOV
Tissue between mesh fibers	Cellularity	Number of mononuclear cells per FOV in increments of 50 cells
	Vascularity	Number of blood vessels per FOV
	Collagen fiber density and thickness	Collagen density as % area of collagen per FOV Collagen fiber thickness as color hue (in order of increasing thickness: green < yellow < orange < red)